VOL. 20, NO. 2-2, 2021, 9-14
www.elektrika.utm.my
ISSN 0128-4428

ELEKTRIKA
Journal of Electrical Engineering

Development of 4D Printed PLA Actuators

Yousif Saad Alshebly[1], **Marwan Nafea**[1*] and **Mohamed Sultan Mohamed Ali**[2]

[1]Department of Electrical and Electronic Engineering, Faculty of Science and Engineering, University of Nottingham Malaysia, 43500 Semenyih, Malaysia.
[2]School of Electrical Engineering, Faculty of Engineering, Universiti Teknologi Malaysia, 81310 UTM Johor Bahru, Johor, Malaysia.

[*]Corresponding author: marwan.nafea@nottingham.edu.my, Tel: +6038924 8168

Abstract: Four-dimensional (4D) printing is currently in the early stages of development and is deficient in offering designers and researchers the freedom to develop 4D printable structures. The first step to ensuring the use of such technology by researchers requires additional testing and simulation for 4D printing. It also requires an assessment of the shape memory effect in the materials that are being printed. This paper tests 4D printed actuators that possess an induced strain following printing. The induced strain is achieved during the printing process following fused deposition modelling. The induced strain permits alteration of the shape after material stimulation following printing, which eliminates the requirement for a separate programming step where alterations are required for force and stimulation to achieve the print shape temporarily. The proposed approach consists of two actuators and a drug delivery application via an open-sided box reservoir. The process of printing and shape change of polylactic acid is completed and the level of bending of actuators is then measured. The printing of designs is done at 10 mm/s for passive layers and 60 mm/s speed for active layers. The heating of the printed samples is done, and the bending angle is measured for the replication process through simulation. Finite element analysis (FEA) of the actuators is done to replicate the strain-induced through the use of materials demonstrating thermal expansion. The FEA parameters are utilized to develop intricate structures and simulate the change of the shape. The deformation values achieved by Designs 1 and 2 in the z-axis are 7.81 mm and 6.06 mm, respectively, and 4.84 mm for the reservoir.

Keywords: 4D printing, actuator, finite element analysis, polylactic acid, shape memory effect.

Article History: received 25 May 2021; accepted 12 June 2021; published 15 September 2021.

1. INTRODUCTION

Three-dimensional printing or additive manufacturing has brought about major changes within the field of prototyping. 3D printing permits the creation of intricate and mechanically functioning elements whilst eliminating the requirement for moulding or pre-processing, which is generally required for traditional forms of manufacturing [1], [2]. This particular form of manufacturing permits printing to order for functional structures, completely eliminating the requirement for stock maintenance. Developments made in additive manufacturing has led to 4D printing, or the usage of smart materials such as shape-memory materials (SMM) in 3D printing [3], [4]. Research into 4D printing is still at its early stages with significant potential for expansion. 4D printing utilizes memory property possessed by certain materials. Such materials possess a definitive change, which can be altered through the use of force or stimuli resulting in newer shapes [5]. The shape memory effect (SME) permits materials to retain an alternate shape and revert back to the original state when a stimulus is applied. Numerous printing methodologies are utilized, ranging from fused deposition modelling (FDM), poly-jetting, digital light printing (DLP) to stereolithography (SLA) [6]. FDM is commonly utilized, where line by line printing is done in a layer-wise manner from a material filament. The wide use of FDM can be attributed to the ease of use of materials.

Thermoplastics used in FDM are materials that undergo melting at a particular temperature while retaining their properties [7]. FDM can be done with shape memory polymers (SMPs) in filament format, which can be simply obtained or produced via a thermal extruder [8]. Numerous materials are utilized for 4D printing depending upon their inherent properties and the potential applications for such. These materials can be regulated through stimuli, where their smart properties can be controlled or activated through different means, either locally or environmentally [9], [10]. The stimuli for such materials can range extensively, whereby common forms include direct heat, light-induced SME, electro-magnetic stimuli, or swellable mediums [11]. Each material has a definitive temperature, which is referred to as glass transition temperature (T_g), where the material transforms from a glassy state to a rubbery state. Temperatures exceeding T_g causes the material to be mendable. Application of force at this stage can cause it to undergo transformation while cooling solidifies the new shape. The initial shape can be simply attained by heating the material beyond the T_g [12], [13]. The most commonly utilized materials in 4D printing are

SMPs, primarily because of the advantageous characteristics shared by them over different smart materials [12]. The SMPS materials shower increased elasticity, a greater difference in Young's modulus between the rubbery and glassy states and lastly ease of manufacturing [14]. Apart from the above mentioned desirable properties, 4D-printed SMP actuators are easy to fabricate when compared to other actuators, such as piezoelectric [15], [16] and pneumatic actuators [17]. These require a complicated fabrication technique to complete.

Owing to the manner in which FDM prints, the printer settings can affect the printed SMP in numerous aspects. Heating the material to melt it and laying it in a definitive manner changes the print, which concurrently results in reheating of the older layers as newer layers are placed on top of them. Multiple studies have been conducted to study the effect of printing parameters on the induced strain of a print [1], [18]–[20]. The speed of printing has an effect on the strain-induced upon the material during the printing. It has been documented that increased printing speeds result in increased strain-induced, resulting in a greater bending rate [18], [19]. The speed of printing in addition to the stored strain within the material also causes the filament to stretch when printing, which results in an increased SME force accumulation within the print. The temperature at which printing occurs also influences the degree of material shrinkage following stimulation after printing. This permits bending by utilizing layers that shrink at multiple rates, thereby causing the development of a strain difference [1]. A low printing temperature results in a greater shrink rate induced in the print. This property can be utilized to print structures having varying printing temperatures for an accurately regulated SME. The print pattern impacts the material bending as the material strain is dependent on the alignment of the patterns [20]. The print pattern impacts the manner and bending direction of the material [1]. Numerous print patterns can be utilized to alter the SME in a particular direction and rate. This particular property, under closed programming, is extremely beneficial for further development of the field. Studies conducted have demonstrated that FDM could be potentially used for printing material which can be used immediately following the printing process. The majority of 4D-printed SMPs structures demand a dedicated programming step where stimulation of the material is done followed by reshaping and cooling in the new shape to achieve SME [21]. This permits structures printed with such properties of pre-strained printing to not require programming, which considerably reduces the time and energy spent. Another added benefit is once the printing process is completed, the structure can be used immediately.

The most common SMP material printed through FDM printers is polylactic acid (PLA). As it is being commonly used for 3D printing, it is utilized in studies as well, the primary reasons being its ease of use and low cost [22]. PLA, being a thermoplastic utilized for FDM, making it a commonly used material in recreational 3D printing. Assessing the response of materials to varying print conditions is done through printing actuators of materials and then analysing the response shown to stimuli. This serves as a platform on which additional improvements and design changes can be done. Actuators permit convenient recording of the printing settings effect on the print, offering accurate data measurements of the SME for simulation. It is difficult to print and analyse complex structures since the complexity of the structure increases the difficulty in replicating it in simulations using accurate designs based on its SME. All these factors contribute to making SME prototyping for applicable structures extremely difficult. Simulations conducted on material response offers an essential threshold level for assessing complex structures, as the simulation settings are formulated on basic testing done on simple structures and the response shown by them to stimuli across varying print settings [1]. The parameters for simulation are to be obtained from the testing done on simple SMP prints, which consists of actuators. The same parameters can then be utilized to test complete designs whilst retaining the material parameters without any change.

In this work, PLA actuator printing and testing is achieved through FDM and is showcased. Sample tests are done to obtain the parameters required for the FEA of the SME. PLA actuator is printed at a predefined rate, layers, and printing temperature. Stimulation of the actuator was done using heating, which activates the SME, resulting in the material to undergo bending. Measurement of the rate of bending is done to assess the parameters required to achieve an equivalent effect in FEA as well. It is vital to conduct FEA following the fabrication step as the properties of the PLA layer are unknown owing to the effect imparted by altering printing speed, temperature and the number of active layers. The results from this are then applied to the simulation of complex structure for potential use in drug delivery.

2. DESIGN AND WORKING PRINCIPLE

The design of the PLA actuators was done to have the following dimensions 30 mm × 1.6 mm × 1 mm (Design 1), and 30 mm × 1.6 mm × 1.2 mm (Design 2) for the length, width, and height, respectively. Individual print layers are 0.1 mm in height with 10 layers of the actuator used in the first sample set and 12 for the second. There are 4 lines of print for each layer. The initial two layers are printed at a rate of 10 mm/s followed by 60 mm/s for the remainder. Previous studies have utilized greater printing speeds, which have shown a direct association between the rate of printing and the induced strain of the material during printing [18]. Printing at lesser speeds minimizes the induced strain, which helps to retain the shape following the printing and activation process. Printing of layers at a significantly low speed permits it to be utilized as a passive layer, permitting greater stored strain gradient between the passive and active layers resulting in a greater actuator bending.

The bending angle of the actuator can be obtained by using the distance between the actuator ends and the deformation distance from the centre of the actuator and the angle formed by the actuator centre at the base. The bending angle calculation is depicted in Figure 1, where the value of A is the distance between the endpoints and B

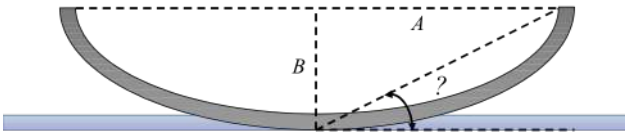

Figure 1. Deformation measurement method of the 4D printed actuators

for deformation of the actuator at the centre. The angle of bending (θ) is calculated using the Pythagoras theorem.

3. FABRICATION AND CHARACTERIZATION

A PLA filament of 1.75 mm diameter and a density of 1.24 g/cm^3 is used for the work (1.75 mm PLA filament 1.0 Kg Gray, Flashforge 3D Technology Co., Ltd., Zhejiang, China), a heated nozzle of 0.4 mm diameter for extrusion and an FDM 3D printer (Ender-3 V2, Creality 3D Technology Co., Ltd., Shenzhen City, China). The room temperature is controlled at 24 °C throughout the printing process. The humidity is regulated together with the temperature and the filament is kept within a dry re-usable bag. In order to achieve an accurate SME for the actuators, three samples are printed from each set, the average value of bending angle and deformation rate is used for further assessment.

Printing small structures was done using a print temperature of 200 °C and bed temperature to 45 °C to achieve improved bed adhesion. The adhesion of PLA material with the print bed permits the actuator to retain the shape during the printing and delay the development of the SME effect till reheating is done following its removal from the print bed. The deformation of the material and its bending is assessed following the stimulation and cooled to a definitive shape. The glass transition temperature for PLA is approximately 60 °C [23]. Hence, to activate the SME of structure, the samples were placed in hot water at 85 °C, which is approximately 25 °C greater than T_g for full heat immersion. This temperature was retained till a complete change of shape was accomplished, following which the samples were left to cool. Alternative heating options for SMPs in the form of directional heating and single-sided heating can result in undesirable bending, which could be restricted to one side. Figure 2(a) showcases the actuator shapes (before and after stimulation), which are based upon Design 1. Figure 2(a) showcases the printed actuators, which were based upon Design 1, right from the printer as well as the actuators following immersion in water at 85 °C, which causes bending in the uppermost print layer.

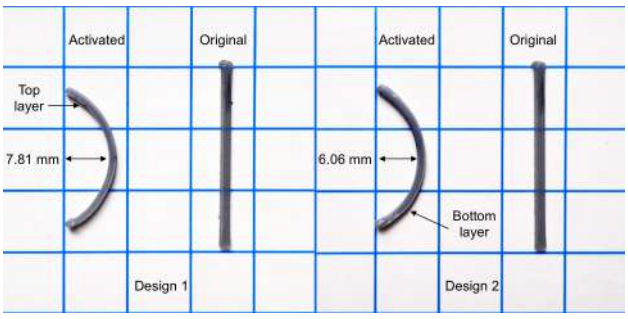

Figure 2. 4D printed actuators before and after stimulation

Once the actuators cool down, the deformation values are measured using a digital calliper (150 mm (6”), precision measuring). The length values between the two ends were found to be 23.02 mm, 22.69 mm, and 21.91 mm, averaging at 22.54 mm. Deformation from the centre of the centre actuator was recorded at 7.02 mm, 8.27 mm, and 8.14 mm, respectively with an average of 7.81 mm. Bending angles were as follows, 31.39°, 36.09°, and 36.61°, at an average of 34.7°. The above measurements should be maintained in the FEA.

The second sample set (Design 2) maintains the same print settings as the first set and has a height of 1.2 mm. Printing of three samples was done followed by immersion in hot water to trigger the SME activation. The length values between the two ends were recorded as 23.37 mm, 23.5 mm, and 22.95 mm, with an average of 23.27 mm. The deformation from the centre of the actuators was recorded at 7.42 mm, 5.43 mm, and 5.34 mm, averaging at 6.06 mm. The bending angles of the three samples were 32.42°, 24.8°, and 24.96°, with an average of 27.39°. Figure 2(b) showcases the actuator shapes as per Design 2 (before and after stimulation). In comparison to the Design 1 actuators seen in Figure 2 (a), the bending seen in Design 2 actuators is lesser as increased thickness results in a lesser degree of bending.

The findings of the experiment can be utilized to predict properties of the material of individual layer, followed by the use of such in the finite element analysis step. Results obtained from this step can be used to effectively when developing advanced structures which would be highlighted in the coming section.

4. FINITE ELEMENT ANALYSIS

As mentioned above, the finite element analysis is an essential step following the fabrication process as the properties of the material of PLA layers are not fully known owing to the influence caused by the alteration of print parameters. ANSYS software (ANSYS, Inc., PA, USA) was utilized for the finite element analysis of PLA actuators. This utilizes a static structural system that permits thermal expansion of the materials utilized in FEA through alteration of varying thermal expansion coefficients ranging from passive (10 mm/s printing speed) and active (60 mm/s printing speed) layers. Selection of the thermal coefficient for the actuators was done by estimation of the parameters resulting in complete actuator shrinkage following SME activation. This permits shrinkage of the entire print whilst estimating the thermal expansion of passive layers, as there is the least shrinkage and minimal stored internal strain within these passive layers. There is a greater internal strain in the active layers, hence requiring a lesser thermal expansion.

Identical actuator designs were used for the simulation, which had the very same dimensions as the printed PLA actuators, but these were subdivided into two separate sections. In the case of Design 1, it was 0.2 mm at the bottom and the remainder was 0.8 mm, these sections were simulated utilizing the individual thermal expansion coefficients (α). Estimation of the α was done through the assessment of the actuator’s deformation distance. The distance was obtained by measuring the length between the

two ends of the actuator and the distance of deformation. It was found that α for the passive layer is -0.004 1/°C and for the active layer is -0.005 1/°C.

Deformation of Design 1 was 7.73 mm, which is on par with the printed actuator shown in Figure 3(a). Hence, displaying an accurate depiction of the SME effect on the alteration of the material's shape. The angle of bending is calculated by taking into account the length between the two ends of the actuator and the deformation seen at the centre of the actuator, which is on par with the printed actuator. In order to further establish the accuracy of the simulation in reproducing SME of printed PLA, a comparison was made with the bending levels seen in Design 2. The simulation done of Design 2 using identical settings revealed an α value for the passive layer is -0.004 1/°C and the α for the active layer is -0.005 1/°C, with changes being made only to the thickness of the actuator. The actuator deformation observed at the centre was 5.68 mm, along with a bending angle similar to the one seen on the printed Design 2 PLA actuators. The following definitively confirmed the accuracy of this particular simulation approach for the SME of PLA. Figure 3(b) showcases the FEA results for Design 2 at a temperature of 80 °C. During the final settings of the simulation process, the PLA actuator which was stimulated by heating showed identical bending to that of the printed actuator, permitting the design and testing of more complex designs, eliminating the prerequisite to print such for additional testing.

The above approach was used once more to assess the effect caused by material properties on bending of a greater surface when exposed to similar settings. The plate was constructed to be 30 mm × 30 mm × 1 mm while retaining 0.2 mm for the passive layer and 0.8 mm for the active layer, as seen in Design 1. The plate is regarded as a unit of design as it shows the same reaction to stimuli without any change and can be then used as the base for alternate structures. The simulation is utilized as proof of concept to analyse the shrinking and bending box, which potentially functions as a reservoir for the drug delivery device [24]. The process of actuation is accomplished by using the box as both top and bottom surfaces in the same composition as that of the actuators. The sidewalls of the box are composed of passive layers. This permits strain to be present amongst the layers only in the z-direction. Therefore, a similar effect would is not seen in the sides of the walls during design simulation. Figure 4 shows the outcomes of the simulation of the active top and bottom of the PLA box. The figure depicts the open-sided box having identical material specifications, which was used for the PLA actuator stimulation. The deformation as masseurs at 4.84 mm for the top and bottom of the reservoir, resulting in a total deformation value of 9.68 mm. The top and bottom of the box used the composition seen in the actuators during the printing process, which lead to high deformation causing a significant reduction of the volume within the box. The sides composed from passive material showed less bending when compared to the top and bottom. The simulation of the SME box was easily achieved as the calculation and matching were done earlier using the PLA actuator.

Temporal deformation occurs in the direction of the z-axis in the proposed designs which are shown in Figure 5. It is evident that the designs achieved steady-state deformation within 5 seconds of stimulation, highlighting the quick response which makes it an ideal option for industrial and biomedical applications. Another important aspect is that the deformation observed in one side of the box was comparatively lower than what was seen in Design 1 (38% lesser) even when the print settings were kept identical for both scenarios. The possible explanation

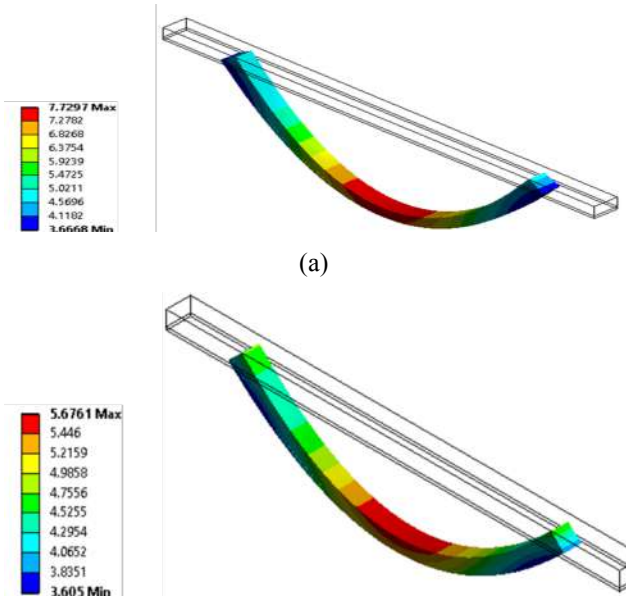

Figure 3. FEA deformation results of the 4D-printed actuators. (a) Design 1. (b) Design 2

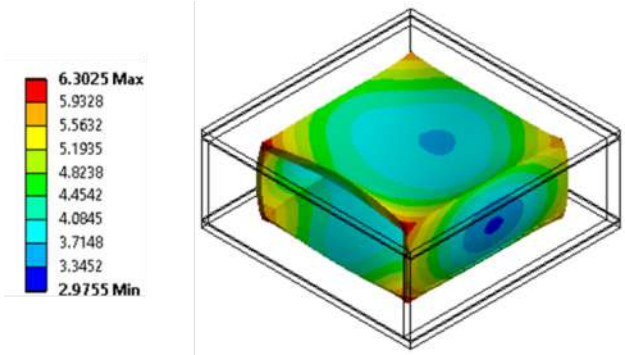

Figure 4. FEA results of the proposed reservoir of drug delivery applications

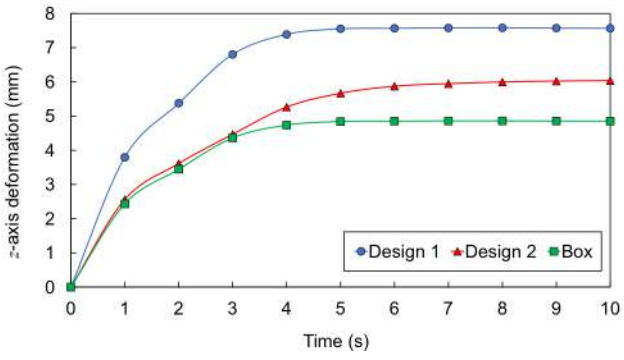

Figure 5. FEA z-axis deformation results of the developed designs

for such being added force is needed for the bending of the sidewalls to occur, which limits complete deformation. The main issue that has to be rectified in the future is minimizing the activation temperature. Active research is being carried out to overcome this issue [25] with slow but steady progress made in this avenue of research. This is particularly important as certain devices should essentially possess low deformation levels to achieve optimal performance of several microliters per minute under operation circumstance when handling low Reynold numbers [26].

5. CONCLUSION

Design tools developed for 4D printed shape memory polymers are immensely useful for researchers to develop new designs. Simulations can be used to project the characteristics exhibited by real printed structures, permitting a simple simulation approach. The methodology presented in this paper offers a simple approach to replicate SME in PLA printed materials. Printing PLA at lesser speeds permits the development of a passive layer having minimal stored strain, whereas printing at high speeds produces an active layer with greater stored strain. The print speeds were 10 mm/s for the passive layer and 60 mm/s for the active layer. This method replicates the SME in PLA through the use of the coefficient of thermal expansion. The coefficient of thermal expansion is -0.004 1/°C and -0.005 1/°C for the passive layer and active layer respectively. Simulation of PLA actuator SME can be done through these settings. The very same settings can be utilized to develop complex structures that could be subjected to testing before proceeding to print. A deformation of 7.81 mm, 6.06 mm, and 4.84 mm in the *z*-axis direction was recorded for Design 1, Design 2, and the reservoir, respectively.

REFERENCES

[1] A. Nojiri, E. Iwase, and M. Hashimoto, "Self-Assembly of Shape Memory Polymer Printed by Fused Deposition Modeling," in *2019 IEEE 32nd Int. Conf. Micro Electro Mech. Syst.*, Seoul, South Korea, Jan. 2019, pp. 380–383.

[2] P. Wang, X. Zheng, J. Li, and B. Zhu, "Prediction of epidemic trends in COVID-19 with logistic model and machine learning technics," *Chaos Solitons Fractals*, vol. 139, p. 110058, Oct. 2020.

[3] Z. Ding, O. Weeger, H. J. Qi, and M. L. Dunn, "4D rods: 3D structures via programmable 1D composite rods," *Mater. Des.*, vol. 137, pp. 256–265, Jan. 2018.

[4] M. R. Abdul Kadir, D. E. O. Dewi, M. N. Jamaludin, M. Nafea, and M. S. Mohamed Ali, "A multi-segmented shape memory alloy-based actuator system for endoscopic applications," *Sens. Actuators, A Phys.*, vol. 296, pp. 92–100, Sep. 2019.

[5] M. H. Ali, A. Abilgaziyev, and D. Adair, "4D printing: a critical review of current developments, and future prospects," *Int. J. Adv. Manuf. Technol.*, vol. 105, no. 1–4, pp. 701–717, Nov. 2019.

[6] J. J. Wu, L. M. Huang, Q. Zhao, and T. Xie, "4D Printing: History and Recent Progress," *Chinese J. Polym. Sci. (English Ed.)*, vol. 36, no. 5, pp. 563–575, 2018.

[7] S. T. Ly and J. Y. Kim, "4D printing – fused deposition modeling printing with thermal-responsive shape memory polymers," *Int. J. Precis. Eng. Manuf. - Green Technol.*, vol. 4, no. 3, pp. 267–272, Jul. 2017.

[8] F. A. Mohd Ghazali, M. N. Hasan, T. Rehman, M. Nafea, M. S. Mohamed Ali, and K. Takahata, "MEMS actuators for biomedical applications: a review," *J. Micromech. Microeng.*, vol. 30, no. 7, p. 073001, Jul. 2020.

[9] L. H. Shao, B. Zhao, Q. Zhang, Y. Xing, and K. Zhang, "4D printing composite with electrically controlled local deformation," *Extrem. Mech. Lett.*, vol. 39, p. 100793, May 2020.

[10] A. Subash and B. Kandasubramanian, "4D printing of shape memory polymers," *European Polymer Journal*, vol. 134. Elsevier Ltd, p. 109771, Jul. 2020.

[11] A. Mitchell, U. Lafont, M. Hołyńska, and C. Semprimoschnig, "Additive manufacturing — A review of 4D printing and future applications," *Addit. Manuf.*, vol. 24, pp. 606–626, Dec. 2018.

[12] X. Kuang *et al.*, "Advances in 4D Printing: Materials and Applications," *Adv. Funct. Mater.*, vol. 29, no. 2, p. 1805290, Jan. 2019.

[13] A. AbuZaiter, O. F. Hikmat, M. Nafea, and M. S. M. Ali, "Design and fabrication of a novel XYθz monolithic micro-positioning stage driven by NiTi shape-memory-alloy actuators," *Smart Mater. Struct.*, vol. 25, no. 10, 2016.

[14] T. Mu, L. Liu, X. Lan, Y. Liu, and J. Leng, "Shape memory polymers for composites," *Compos. Sci. Technol.*, vol. 160, pp. 169–198, May 2018.

[15] S. A. M. Rifai, M. Nafea, S. K. Debnath, and S. Bagchi, "Hybrid Hysteresis-Inversion and PSO-Tuned PID Control for Piezoelectric Micropositioning Stages," in *2020 IEEE Stud. Conf. Res. Dev.*, Batu Pahat, Malaysia, Sep. 2020, pp. 206–210.

[16] M. Nafea, A. Nawabjan, and M. S. Mohamed Ali, "A wirelessly-controlled piezoelectric microvalve for regulated drug delivery," *Sens. Actuators, A Phys.*, vol. 279, pp. 191–203, Aug. 2018.

[17] T. Rehman, M. Nafea, A. A. Faudzi, T. Saleh, and M. S. M. Ali, "PDMS-based dual-channel pneumatic micro-actuator," *Smart Mater. Struct.*, vol. 28, no. 11, p. 115044, Nov. 2019.

[18] L. Kačergis, R. Mitkus, and M. Sinapius, "Influence of fused deposition modeling process parameters on the transformation of 4D printed morphing structures," *Smart Mater. Struct.*, vol. 28, no. 10, p. 105042, Sep. 2019.

[19] R. Noroozi, M. Bodaghi, H. Jafari, A. Zolfagharian, and M. Fotouhi, "Shape-adaptive metastructures with variable bandgap regions by 4D printing," *Polymers (Basel).*, vol. 12, no. 3, 2020.

[20] A. Zolfagharian, A. Kaynak, S. Y. Khoo, and A. Kouzani, "Pattern-driven 4D printing," *Sens. Actuators, A Phys.*, vol. 274, pp. 231–243, May 2018.

[21] F. Momeni, S. M.Mehdi Hassani.N, X. Liu, and J. Ni, "A review of 4D printing," *Mater. Des.*, vol. 122, pp. 42–79, May 2017.

[22] M. Carlson and Y. Li, "Development and kinetic evaluation of a low-cost temperature-sensitive shape memory polymer for 4-dimensional printing," *Int. J. Adv. Manuf. Technol.*, vol. 106, no. 9–10, pp. 4263–4279, Feb. 2020.

[23] J. Wang, Z. Wang, Z. Song, L. Ren, Q. Liu, and L. Ren, "Programming Multistage Shape Memory and Variable Recovery Force with 4D Printing Parameters," *Adv. Mater. Technol.*, vol. 4, no. 11, p. 1900535, Nov. 2019.

[24] M. Nafea, A. AbuZiater, O. Faris, S. Kazi, and M. S. Mohamed Ali, "Selective wireless control of a passive thermopneumatic micromixer," in *2016 IEEE 29th Int. Conf. Micro Electro Mech. Syst.*, Shanghai, China, Jan. 2016, pp. 792–795.

[25] A. Bajpai, A. Baigent, S. Raghav, C. Ó. Brádaigh, V. Koutsos, and N. Radacsi, "4D Printing: Materials, Technologies, and Future Applications in the Biomedical Field," *Sustainability*, vol. 12, no. 24, p. 10628, Dec. 2020.

[26] M. Nafea, M. S. M. Ali, T. Rehman, and K. Mehranzamir, "Geometrical Analysis of Diffuser-Nozzle Elements for Valveless Micropumps," in *2019 IEEE Int. Conf. Smart Instrumentation, Meas. Appl.*, Kuala Lumpur, Malaysia, Aug. 2019, pp. 1–5.